Basics of GM Counter-Characteristics and Counting Statistics

Gayatri P
3rd year, Integrated M.Sc. Physics
Roll No.: 2211185
(Dated: April 1, 2025)

In this experiment, we use the Geiger-Muller (GM) counter to study the quantification of radioactivity. We first determine the the characteristics of a GM Counter and find its operating frequency for both a β and a γ source. We then verify the inverse square law relation of count rates with distance. We also calculate the activity of Cs-137 and hence efficiency of the GM counter. Furthermore, we also analyse counting statistics and verify that for a large number of measurements, our count distribution resembles a normal distribution.

I. THEORY

The Geiger-Müller (GM) counter is a radiation detection device used to measure ionizing radiation, such as alpha, beta, and gamma rays. It operates by detecting the ionization produced by radiation in a gas-filled tube, leading to an electrical pulse that is counted and displayed. GM counters are widely used in radiation safety monitoring, environmental surveys, nuclear industry applications, medical radiation detection, and laboratory research. Their high sensitivity to radiation and ease of use make them valuable tools for detecting and measuring radiation levels in various settings.

The Geiger-Muller (GM) counter works by detecting the ion-electron pairs created by the interaction of charged particles in a gas mixture. The GM tube is a metal cylinder with a thin wire (anode) at its axis and a metal cylinder (cathode) maintained at a high voltage to create an electric field. The radiation enters through a window on the tube, creating ion-electron pairs that are swept by the electric field to produce a phenomenon called an avalanche, which generates output pulses that are counted by related circuits. A schematic diagram of the GM counter is shown in Fig. II.

As shown in Fig. I the operating voltage of the GM counter is set in the plateau region, where the counting rate is relatively constant. The plateau length and slope determine the stability of the counting rate, while the dead time, resolving time, and recovery time limit the counting rate. The GM counter is insensitive to ionizing events during the dead time, and the resolving time and recovery time set the minimum time interval between two distinct and normal-size pulses, respectively. Higher voltages and the gas composition inside the GM tube can reduce the effects of these factors. The background counting rate can be due to cosmic rays, electronic noise or other active sources in the same room.

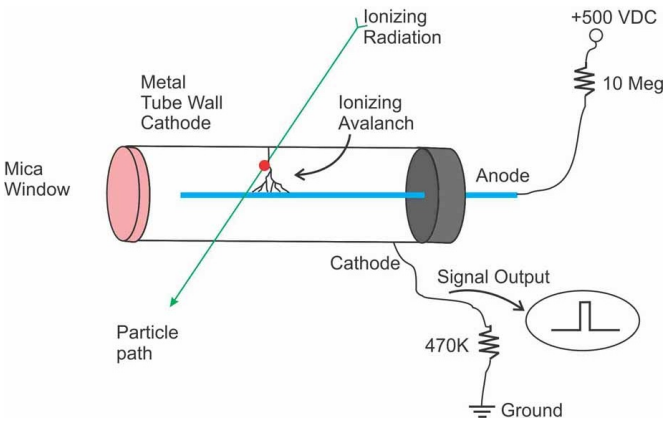

FIG. 1: Schematic setup of a GM Counter

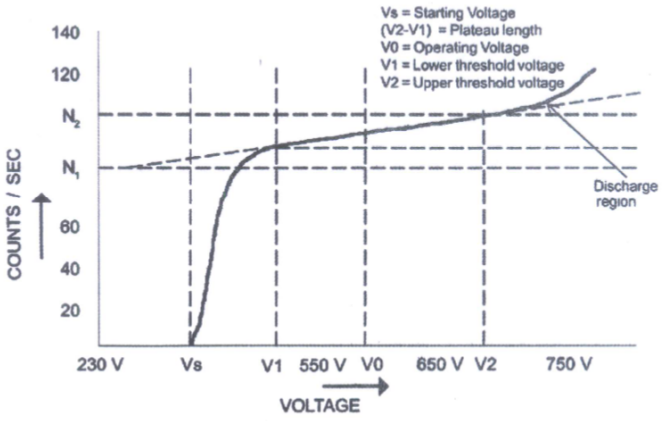

FIG. 2: Typical voltage characteristics of a GM Counter

A. Inverse Square Law

It states that the gamma radiations reduce inversely proportional to the distance, d, between the detector and the radiation source. Thus, the counting rate, R (counts/second), should be related as follows,

$$R \propto \frac{1}{D^2}$$
$$\therefore \log(R) = -2 \times \log(D) + C \quad (1)$$

where C is some constant.

B. Efficiency of GM counter

If the current activity of a radioactive source is denoted as A, the fraction of emitted gamma radiation that enters the GM tube is given by:

$$R = A \times \frac{\pi d^2/4}{4\pi D^2} = A \times \frac{d^2}{16D^2} \tag{2}$$

where D is the distance from source to the end window and d is the diameter of the end window. The activity of a radioactive substance follows the exponential decay law:

$$A = A_0 e^{-\lambda t} \tag{3}$$

where A_0 represents the initial activity, λ is the decay constant, and t is the elapsed time.

$$\lambda = \frac{\ln(2)}{T_{\text{half}}} \tag{4}$$

The efficiency (E) of a GM detector for gamma radiation is defined as the ratio of the counts per second (CPS) to the disintegrations per second (DPS), which is expressed as:

$$E = \frac{\text{CPS}}{\text{DPS}} = \frac{N}{R} \tag{5}$$

C. Counting Statistics

Say N_i denote the i^{th} reading of a measurement in a set of n measurements, then the equations for calculating mean ($\bar{N}$), variance σ^2, and standard deviation σ (for large samples, as dictated by the law of large numbers) are:

$$\bar{N} = \frac{1}{N}\sum_{i=1}^{n} N_i \tag{6}$$

$$\sigma^2 = \frac{1}{n}\sum_{i=1}^{n} (\bar{N} - N_i) \tag{7}$$

II. EXPERIMENTAL SETUP

Apparatus

1. Cesium-137 (Gamma Source)
2. Thalium-204 (Beta Source)
3. GM counting System
4. GM detector
5. Sliding Bench
6. Detector Stand
7. BNC cable

Fig. III shows and labels all used apparatus in this experiment.

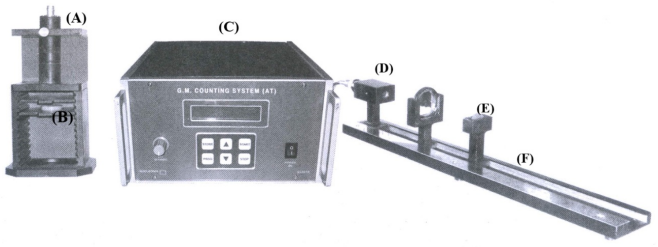

FIG. 3: Experimental Setup where (A) and (B) are the end window detector and source holder (C) is the GM counting system where you can vary the EHT (D) and (E) are the end window detector and source holders attached to a (E) sliding bench

III. OBSERVATION AND CALCULATIONS

A. GM Characteristics

For the characteristics of GM Counter, the GM counter was kept in the detector stand. The γ-source was kept at a distance of 2 cm while the β-source was kept at a distance of 4 cm from the detector.The EHT voltage of the detector was varried and the number of counts was noted for 30s. For each voltage setting, the source was removed and background radiation counts was also taken. The results tabulated in Table II and I (All observational data is presented in the appendix) and are plotted (Figs. 4 and 5) and discussed below.

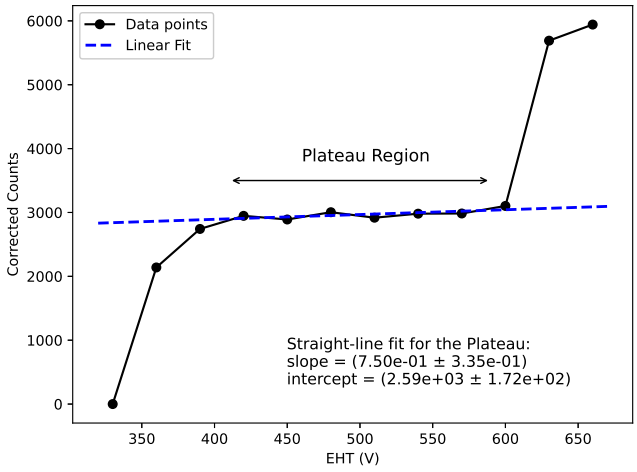

FIG. 4: GM characteristics for γ-source Cs-137

From Fig. 4, the starting voltage of plateau is $V_1 = 420$ V and the ending voltage for the plateau is $V_2 = 600$ V. The plateau length is $(600 - 420) = 190$ V. The operating voltage is hence $V_0 = 510$ V. Doing least square fitting for a straight line on the slope, the slope of the plateau is (0.75 ± 0.36) and the intercept is (2592 ± 172).

The percentage slope of the plateau is given by,

$$\begin{aligned} \%\ \text{slope} &= \frac{N_2 - N_1}{N_1} \times \frac{100}{V_2 - V_1} \times 100 \qquad (8) \\ &= 2.92\% \end{aligned}$$

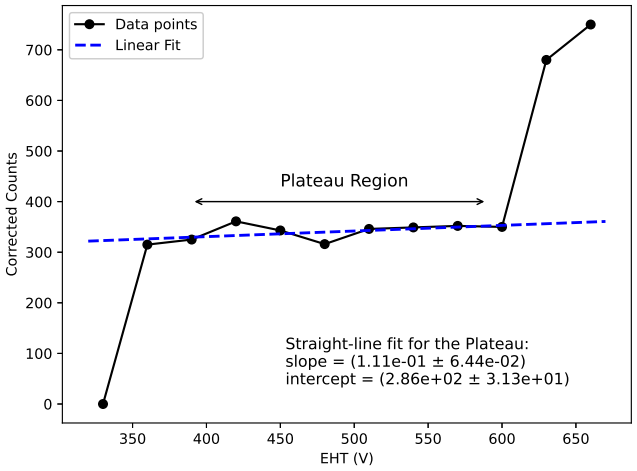

FIG. 5: GM characteristics for β-source Tl-204

From Fig. 5, the starting voltage of plateau is 390 V and the ending voltage for the plateau is 600 V. The plateau length is $(600-390) = 210$ V. The operating voltage is hence 495 V. Doing least square fitting for a straight line on the slope, the slope of the plateau is (0.11 ± 0.06) and the intercept is (286 ± 31).

The percentage slope is given by Eq. 8 as was found to be 3.66%.

B. Inverse Square Law Relation

EHT voltage is now fixed at 510V and the counting time is 60s. By using the γ-source, obtained counts (for 60s) for the source placed at different distances d from the detector (Table III). The corrected counts have be calculated using Table IV.

Fitting the R vs. d plot (Fig 6) using a function of the form $R = A + B/d^2$, the values of A and B obtained are shown in the figure.

When the corrected count rate R is plotted vs. d by taking the log in both axes, we get Fig. 7. In Fig. 7, the slope of the line indicates the exponent of d w.r.t. R, which should ideally be equal to -2 (Eq. 1). Here, have obtained a slope of $-(1.60 \pm 0.05)$.

This means there is a significant source of error in our observations, leading to a small deviation in the inverse-square relation between count rates and distance.

We can also plot R vs. $1/d^2$ to observe how closely it follows a straight line. The resultant plot and the parameters are shown in Fig. 8.

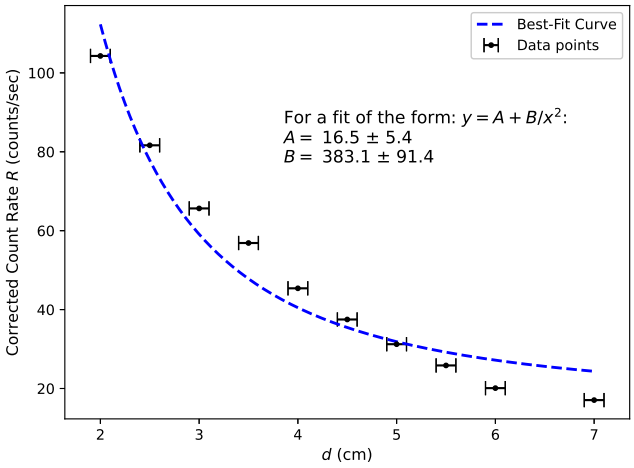

FIG. 6: Variation of Count Rate R with distance d for γ-source Cs-137

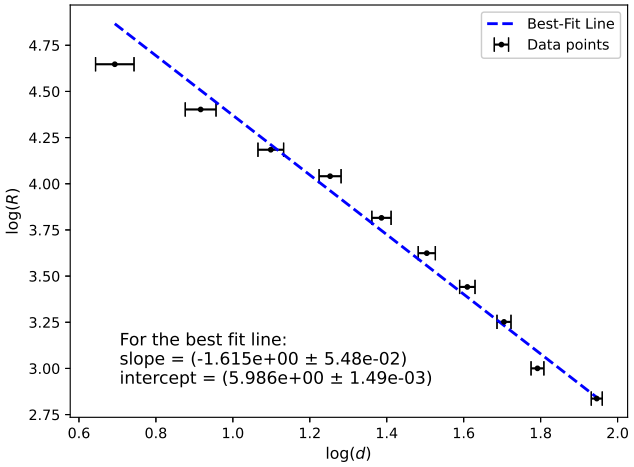

FIG. 7: Variation of Count Rate R with distance d for γ-source Cs-137 in the log scale

C. Efficiency of Detection

For a Cesium-137 source, where the initial activity in May 2016 was $A_0 = 86$ kBq, the decay constant is determined using Eq. 4. Given that the half-life of Cesium-137 is $T_{\text{half}} = 30.17$ years, we can compute λ as,

$$\lambda = \frac{\ln(2)}{30.17} \approx 0.02297 \text{ year}^{-1}$$

and the elapsed time from May 2016 to March 2025 is:

$$t = 2025 - 2016 + \frac{9 \text{ months}}{12 \text{ months/yr}} = 8.75 \text{ years}$$

Substituting these values into the decay equation, we get the activity of the Cesium-137 source at the given time

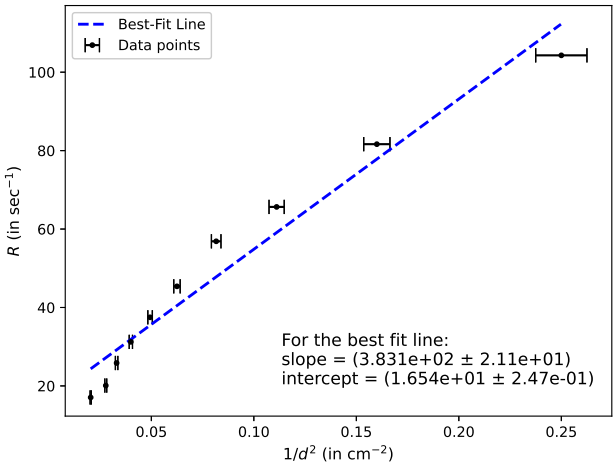

FIG. 8: Variation of Count Rate R with $1/d^2$ for γ-source Cs-137

to be,

$$A = 86 \times e^{-0.02297 \times 8.75}$$
$$\approx 70.47 \text{ kBq}$$

Using this estimated activity for Cs-137 in March 2025, we can substitute this into Eq. 5 along with $D = 10$ cm and $d = 1.5$ cm to obtain $R = 99.098$ s^{-1}. This is the fractional radiation entering the detector.

Given the net count rate $N = 14.711$ s^{-1} (from Table V), the efficiency can be calculated as:

$$E = \frac{14.711}{99.098} \times 100 = 14.84\%$$

D. Nuclear Statistics

1. *Background Statistics*

After removing the radioactive source from the source holder we have taken two sets of 10 readings each of the background noise with the set the preset time to 10s and 100s (Table VI) respectively (EHT = 510 V). The bar graph for number of counts registered versus the Index Number has been shown in Fig. 9.

By comparing the two plots in Fig. 9, we can deduce that the spread in measured values decreases as the number of pulses registered increases. Hence, the background noise reaches a stable value and shows less variation as the measurement time increases.

Now, to further demonstrate the point, we we have repeated the measurement 50 time with time of measurement 100s each. The results are tabulated in Table VIII. Fig. 10 shows the spread in the background counts. From this distribution, we can find the statistical parameters for the background counts as follows.

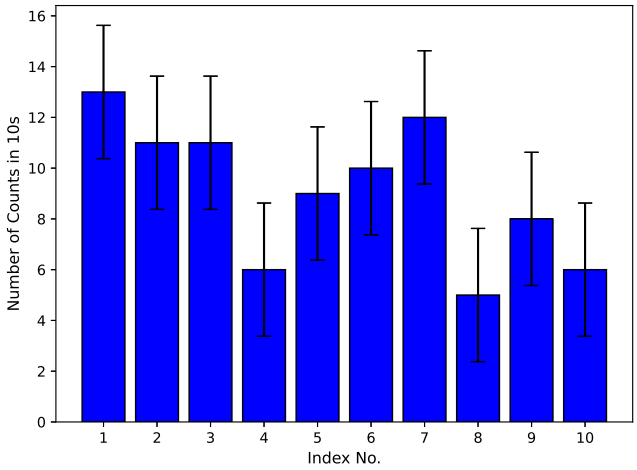

(a) 10 seconds ($\sigma = 2.62$)

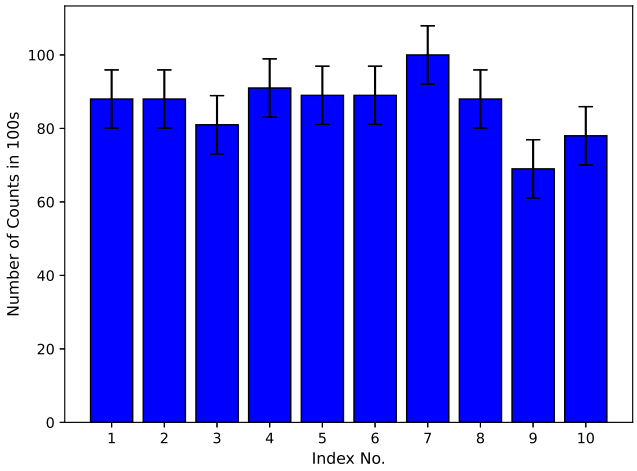

(b) 100 seconds ($\sigma = 7.93$)

FIG. 9: Measurement of the background count for different lenghts of time. The error bars show the standard deviation in the measurements. We can see that the relative spread decreases as the measurement time increases.

- Mean:

$$\bar{N} = \frac{4432}{50} \approx 89 = 0.89 \text{ counts/sec}$$

- Variance:

$$\sigma^2 = \frac{1}{N}\sum_{i=1}^{N}(N_i - \bar{N})^2$$
$$= \frac{4467.52}{50} = 89.35$$

- Standard deviation:

$$\sigma = \sqrt{89.35} = 9.45$$
$$= 0.09 \text{ counts/sec}$$

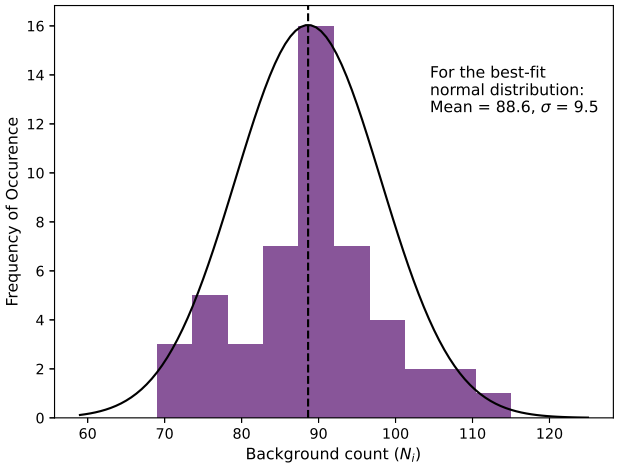

FIG. 10: Distribution of background counts overlaid with a normal fitting function

Here, all values have been divided by 100s to get the count rates.

2. *Distribution of Decay Counts*

For studying the number statistics, the β-source is kept at a distance of 2 cm from the detector and the counts were recorded for 25s at fixed EHT voltage of 510 V. The readings are tabulated in Table VII.

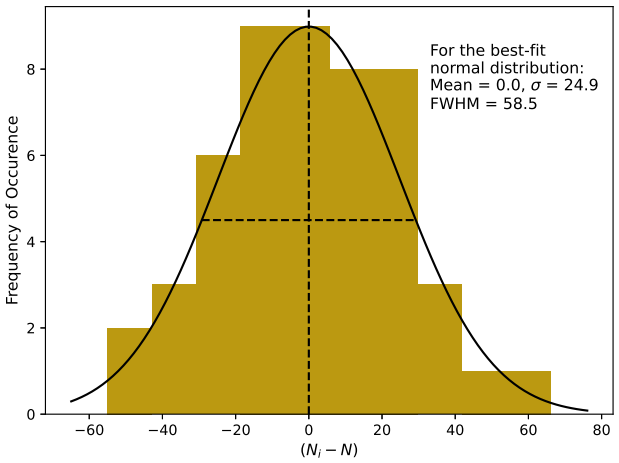

FIG. 11: Distribution of $(N_i - N)$ for β-source, where N is the mean value

From Fig. 11, we can see that the distribution tends to be Gaussian distribution as the number of measurements performed is increased. The distribution is also symmetric about the mean value. The parameters for the best-fit Gaussian distribution are shown in the figure. The mean value for $(N_i - \bar{N})$ obtained is 0 as expected. The standard deviation was obtained to be $\sigma = 24.9 \approx \sqrt{\bar{N}}$, where $\bar{N}$ is the mean value of the counts which was measured to be 632.92.

Because the mean value is large, the adjacent values of the function are not greatly different from each other. i.e., the distribution is slowly varying which is the expected behavior of a normal distribution.

IV. ERROR ANALYSIS

For the error in Plateau Slope percent in GM Characteristics, we can calculate (for the γ-source),

$$\Delta(\%\text{ slope}) = \frac{\Delta\text{slope}}{\text{slope}} - \frac{\Delta N}{N} \tag{9}$$
$$= \frac{3.35}{7.50} - \frac{64}{2975} = 0.43$$
$$\therefore \%\text{ plateau slope} = (2.92 \pm 0.43)\%$$

Similarly for the β-source

$$\Delta(\%\text{ slope}) = \frac{0.64}{1.11} - \frac{14}{363} = 0.54$$
$$\therefore \%\text{ plateau slope} = (3.66 \pm 0.54)\%$$

For efficiency, we can assume that the error in DPS is negligible. Now, the standard deviation of the CPS in Cs-137 is 0.217. Thus, uncertainity in efficiency will be measured similarly using error propagation as,

$$\Delta\text{Eff}_{\text{Cs}} = 14.84 \times \frac{0.217}{14.711} = 0.22\%$$

V. DISCUSSION & CONCLUSION

We have successfully characterised the GM counter in this experiment and studied the statistics of decay counting.

We observed a plateau in the GM characteristic curve obtained by varying operating voltage and measuring the counts. When using γ-source, we observed that the threshold voltages are 390V and 600V. The operating voltage is 510 V and the percentage slope of the plateau is $(2.92 \pm 0.43)\%$. For the β-source, the threshold voltages are 390 V and 600 V. The operating voltage is 485 V and the percentage slope of the plateau is $(3.66 \pm 0.54)\%$. The GM counter must operated in this plateau so that little fluctuations in the EHT voltage do not impact the number of counts.

In the second part of the experiment, we varied the distance between the source and the detector and measured the count rates. We verified the inverse square relation between the count rate and the distance from the source and the detector. By plotting count rate and distance in the log scale, we found out that the experimentally observed relation was of the form count rate $\propto d^{-(1.62 \pm 0.05)}$.

The significant source of error could mainly be due to the error in the distance measured by eye.

We then measured the efficiency of the GM counter, which, for the γ-source came out to be $(14.84 \pm 0.22)\%$. The efficiency the measurement process is governed by the distance between the source and the detector as well as the detector window size. The current activity of the source also affects the efficiency of the detector.

Furthermore, we also studied the statistics of the GM counter. We observed that the relative spread in background count decreases as the measurement time increases. By taking a large amount (50) background count readings (with a measurement time of 100s), we determined the mean and standard deviation of the background count rate to be (0.89 ± 0.09) counts/sec.

Next, we studied the statistics of β decay count values by collection 50 different data points. The observed counts followed a Gaussian distribution around a mean value, underscoring the need for statistical analysis in interpreting experimental data.

VI. PRECAUTIONS AND SOURCES OF ERROR

1. Unintended variations in source orientation: The use of disk-shaped radioactive sources without knowing the proper side could introduce inconsistencies in the data. The two flat surfaces of the disk may have different emission characteristics.
2. The use of a small sample size of 50 data points for the counting statistics part of the experiment may not fully represent the underlying distribution of counts. Ideally 1000 or more measurements are required to properly approach a Gaussian distribution, as dictated by the *law of large numbers*.
3. The distances measured on the grove could have human error such as parallax asoociated with them, along with incorrect assumption of where exactly the detector/source is placed on the scale.

Appendix A: Observational Data

1. GM Characteristics

Potential (V)	Count	Background	Corrected Counts
330	0	0	0
360	2161	22	2139
390	2777	35	2742
420	2977	30	2947
450	2915	25	2890
480	3039	35	3004
510	2949	31	2918
540	3016	35	2981
570	3029	45	2984
600	3140	38	3102
630	5738	48	5690
660	6022	80	5942

TABLE I: GM characteristic data for the γ-source

Potential (V)	Count	Background	Corrected Counts
330	0	0	0
360	337	22	315
390	360	35	325
420	391	30	361
450	368	25	343
480	351	35	316
510	377	31	346
540	384	35	349
570	397	45	352
600	388	38	350
630	728	48	680
660	830	80	750

TABLE II: GM characteristic data for the β-source

2. Inverse Square Law Relation

Distance (d) (cm)	Count	Corrected Count in 60s	Count Rate/sec (R)
2.0	6321	6257.6	104.293
2.5	4962	4898.6	81.643
3.0	4002	3938.6	65.643
3.5	3476	3412.6	56.877
4.0	2787	2723.6	45.393
4.5	2313	2249.6	37.493
5.0	1937	1873.6	31.227
5.5	1614	1550.6	25.843
6.0	1269	1205.6	20.093
7.0	1087	1023.6	17.060

TABLE III: Count rates measured at different values of d

Background Count (in 60s)	Average Background Count (for 60s)
71	
53	
74	63.4
57	
62	

TABLE IV: Count rates measured at different values of d

3. Efficiency of Detection

Counts	BG Counts	Mean BG Count	Corr. Counts per second (CPS)	Std. Dev. (σ_{CPS})
978	117			
1007	96	106	14.711	0.217
981	105			

TABLE V: Count data (for 60s) for efficiency of detector for the γ-source

4. Nuclear Statistics

S.No.	Count (for 10s)	Count (for 100s)
1	13	88
2	11	88
3	11	81
4	6	91
5	9	89
6	10	89
7	12	100
8	5	88
9	8	69
10	6	78
Mean	9.10	86.10
Std. Dev.	2.61	7.89

TABLE VI: Background counts observed for different measuring times

N_i	$N_i - N$	$(N_i - N)^2$	N_i	$N_i - N$	$(N_i - N)^2$
88	-0.64	0.41	74	-14.64	214.33
88	-0.64	0.41	92	3.36	11.29
81	-7.64	58.37	88	-0.64	0.41
91	2.36	5.57	69	-19.64	385.73
89	0.36	0.13	89	0.36	0.13
89	0.36	0.13	90	1.36	1.85
100	11.36	129.05	74	-14.64	214.33
88	-0.64	0.41	101	12.36	152.77
69	-19.64	385.73	90	1.36	1.85
78	-10.64	113.21	83	-5.64	31.81
102	13.36	178.49	80	-8.64	74.65
97	8.36	69.89	106	17.36	301.37
84	-4.64	21.53	89	0.36	0.13
102	13.36	178.49	86	-2.64	6.97
92	3.36	11.29	97	8.36	69.89
91	2.36	5.57	106	17.36	301.37
87	-1.64	2.69	81	-7.64	58.37
88	-0.64	0.41	74	-14.64	214.33
85	-3.64	13.25	93	4.36	19.01
115	26.36	694.85	88	-0.64	0.41
87	-1.64	2.69	78	-10.64	113.21
89	0.36	0.13	90	1.36	1.85
94	5.36	28.73	96	7.36	54.17
73	-15.64	244.61	95	6.36	40.45
93	4.36	19.01	83	-5.64	31.81

TABLE VII: Background counts observed with measuring time 100s each

N_i	$N_i - N$	$(N_i - N)^2$	N_i	$N_i - N$	$(N_i - N)^2$
646	13.08	171.09	604	-28.92	836.37
672	39.08	1527.25	628	-4.92	24.21
639	6.08	36.97	634	1.08	1.17
637	4.08	16.65	618	-14.92	222.61
660	27.08	733.33	655	22.08	487.53
605	-27.92	779.53	597	-35.92	1290.25
656	23.08	532.69	626	-6.92	47.89
630	-2.92	8.53	628	-4.92	24.21
615	-17.92	321.13	598	-34.92	1219.41
631	-1.92	3.69	656	23.08	532.69
634	1.08	1.17	585	-47.92	2296.33
640	7.08	50.13	616	-16.92	286.29
578	-54.92	3016.21	623	-9.92	98.41
603	-29.92	895.21	617	-15.92	253.45
699	66.08	4366.57	634	1.08	1.17
607	-25.92	671.85	659	26.08	680.17
656	23.08	532.69	639	6.08	36.97
666	33.08	1094.29	659	26.08	680.17
623	-9.92	98.41	634	1.08	1.17
647	14.08	198.25	641	8.08	65.29
666	33.08	1094.29	626	-6.92	47.89
608	-24.92	621.01	644	11.08	122.77
621	-11.92	142.09	656	23.08	532.69
613	-19.92	396.81	646	13.08	171.09
593	-39.92	1593.61	678	45.08	2032.21

TABLE VIII: Counts observed for the β-source with measuring time 25s each

[1] *G.M. Counting System: User Manual*, Nucleonix Systems Pvt. Ltd. (2022).

[2] M. M. Bé and V. Chisté, Table of radionuclides (vol. 3 to 244) (2006).